Spatial distribution of cell collapse in *Eucalyptus nitens* wood due to drying treatment

Alan Dickson and Rosie Sargent

Date: May 2021

Report: SWP-T125

Report information sheet

Report title	Spatial distribution of cell collapse in *Eucalyptus nitens* wood due to drying treatment
Authors	Alan Dickson and Rosie Sargent Scion
PAD output number	35394345
Signed off by	Name of person signing off report
Date	May 2021
Confidentiality requirement	Confidential (for client use only)
Intellectual property	
Disclaimer	The information and opinions provided in the Report have been prepared for the Client and its specified purposes. Accordingly, any person other than the Client uses the information and opinions in this report entirely at its own risk. The Report has been provided in good faith and on the basis that reasonable endeavours have been made to be accurate and not misleading and to exercise reasonable care, skill and judgment in providing such information and opinions. Neither Scion, nor any of its employees, officers, contractors, agents or other persons acting on its behalf or under its control accepts any responsibility or liability in respect of any information or opinions provided in this Report.

Published by: Scion, Private Bag 3020, Rotorua 3046, New Zealand. www.scionresearch.com

TABLE OF CONTENTS

CONTENTS

Abstract

This work is part of a broader approach to characterising and understanding the mechanisms of cell collapse and within-ring checking in hardwoods during drying. Understanding the causes of such timber degrade gives us options for dealing with it in the future, such as identifying collapse-prone timber prior to drying, or developing drying methods that avoid the conditions that cause checking and collapse. In this microscopy approach we characterise and measure collapse and checking responses, and spatial relationships, at a cellular level but can do this over a size scale closer to which they occur and are an issue during timber processing. A conventional, stereo light microscope was used to image polished wood surfaces. This was done at cellular resolution, over size-scales of the growth-ring or larger. An image analysis approach was developed that enabled cell collapse to be identified, located and measured. The analysis of air, kiln, and oven-dried *Eucalyptus nitens* showed that cell collapse was highly variable but generally more prominent in the outer third of growth rings. There were significant changes in vessel shape across the growth-rings and vessel area was significantly reduced by drying. The technique provides an intermediate step between detailed microscopy and macroscopic imaging that allows spatial analysis at the wood cell level. The result is the detailed imaging and analysis of cell collapse and its relationships to wood morphology and the major hydraulic pathways. This will allow for the investigation of cell collapse and checking mechanisms and how they related to the broader growth ring and wood morphology and structure.

Spatial distribution of cell collapse in *Eucalyptus nitens* wood due to drying treatment

Introduction

Cell collapse is a common issue during the drying of many woody species (Kauman, 1960), and is often a limiting factor for utilising these species for sawn timber. The purpose of this work is to provide an approach to imaging woody materials over large regions of interest that allows for the measurement and spatial analysis of cell collapse and deformation due to drying. *Eucalyptus nitens*, which makes up a small percentage of the exotic plantation but has a good growth rate and shows economic potential within New Zealand (Satchell, 2016), was evaluated. A conventional, stereo light microscope fitted with a motorized XY stage, was used to directly image polished wood samples. The goal was to determine if the stereo microscope gave sufficient cell detail over large areas for successful image analysis. Of particular interest were that the setup was able to determine significant differences in *E. nitens* morphology (cell shape and arrangements) due to drying treatments.

Microscopic analysis of woody samples is generally limited to small regions of interest constrained by the field of view of the microscope lens and the difficulty in preparing large samples. However, imaging at high resolution over large areas is sometimes required where spatial relationships, outside the microscope's field of view, are being investigated. For example, when investigating cambial dynamics in *Pinus radiata*, images with a dimension >2mm were routinely required to fully capture the cambial zone (Dickson, *et al*., 2017; Nanayakkara, *et al*., 2019). It was also identified that imaging over large areas is required to understand the cell dimension changes due to wood drying in *Eucalyptus nitens* (Dickson & Dawson, 2020). In such cases overlapping images and image stitching to form a single mosaic image are required and algorithms are available to achieve this (Preibisch, *et al*., 2009).

Materials and methods

Material

The morphological changes due to drying were evaluated on 24 boards of *Eucalyptus nitens* (H. Deane & Maiden). The board samples were produced for a previous study (Dawson, *et al.*, 2020). Wood from eight trees of *E. nitens* was cut into 37 × 37 × 200 mm boards. The boards were either air-dried at 25°C/65% relative humidity (RH), which is equivalent to 12% equilibrium moisture content (EMC); oven-dried at 103°C until a constant mass was reached, or kiln-dried using a kiln schedule (70°C/65°C). More details of the wood material and the kiln-drying schedule are given in Dawson *et al.* (2020). After drying treatment, a 5 mm thick sub-sample was cut from the middle of each of the 200 mm long boards. These sub-samples (approximately 37 × 37 × 5 mm – depending on shrinkage) were then prepared for microscopy.

Sample preparation

A white, oil-based paint was used to fill the cell lumens and provide contrast with the cell walls for image analysis. The transverse surface was sanded using a 320-grit paper to expose the wood surface beneath the paint. It was then polished using an 800-grit paper to remove scratches.
A stereo microscope with a motorized XY scanning stage was used to image the polished wood surface at cell resolution (a total of 1760 images) and stitch the images together using freeware (ImageJ).

Image analysis was limited to a single growth-ring within the image so comparisons could be made at the growth-ring level using an area of approximately 13.9 × 13.9 mm. Each point within the growth-ring could be assigned a position relative to the growth-ring boundaries.
Example images from macro to micro-level of the same sample of an *E. nitens* board are shown in Figure 1. Further details used to determine features are shown in Figure 2.

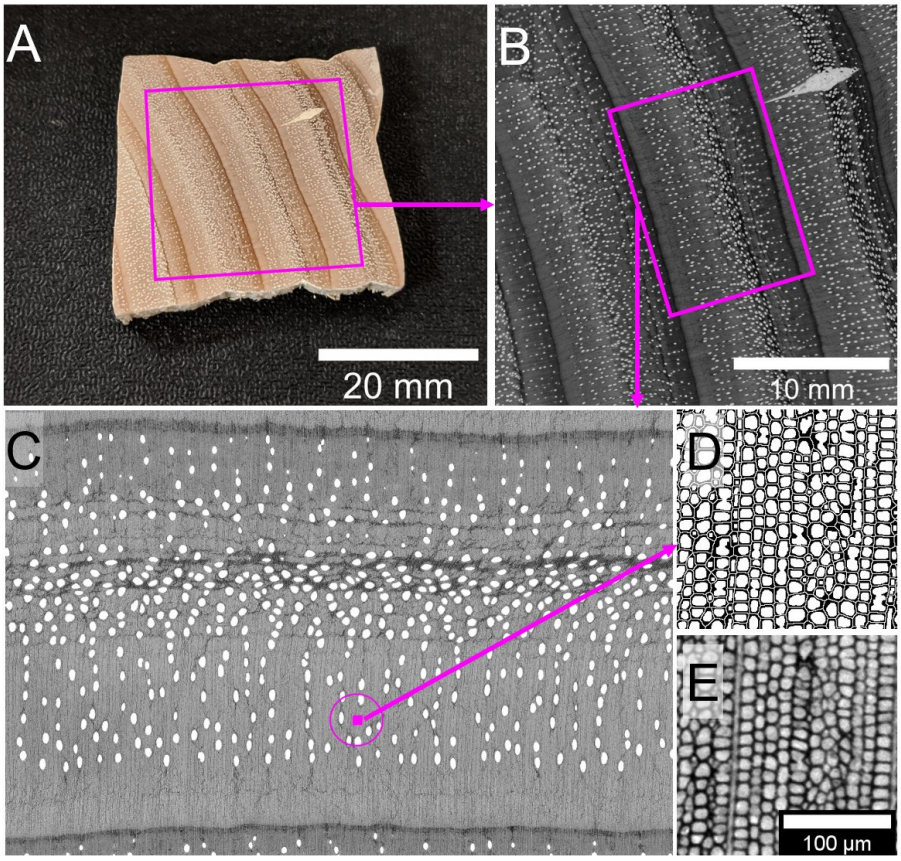

Figure 1. Overview (oven-dried sample of *E. nitens* board). (A) Filled (paint) and polished sample. (B) Imaged region after stitching. (C) Binarised image of selected growth-ring. (D) Detail of the binarized image showing cell perimeters. (E) Corresponding greyscale image.

Vessels were identified by automatic thresholding. Cell collapse was estimated from the cell wall thickness map. In Figure 2A, collapsed cells appear dark and because cell lumens are not present, cells are generally not detected (Fig. 2B). Therefore, these appear to be regions of high wall thickness (actually, the distance between detectable cell lumens) (Fig. 2C).

Analysis was performed with R (version 4.0.3) (R Core Team 2020) using RStudio (Version 1.3.1093) (RStudio Inc, Boston, MA, USA). Analysis and presentation primarily used "dplyr" (Wickham, *et al.*, 2019) and "ggplot2" (Wickham, 2016)

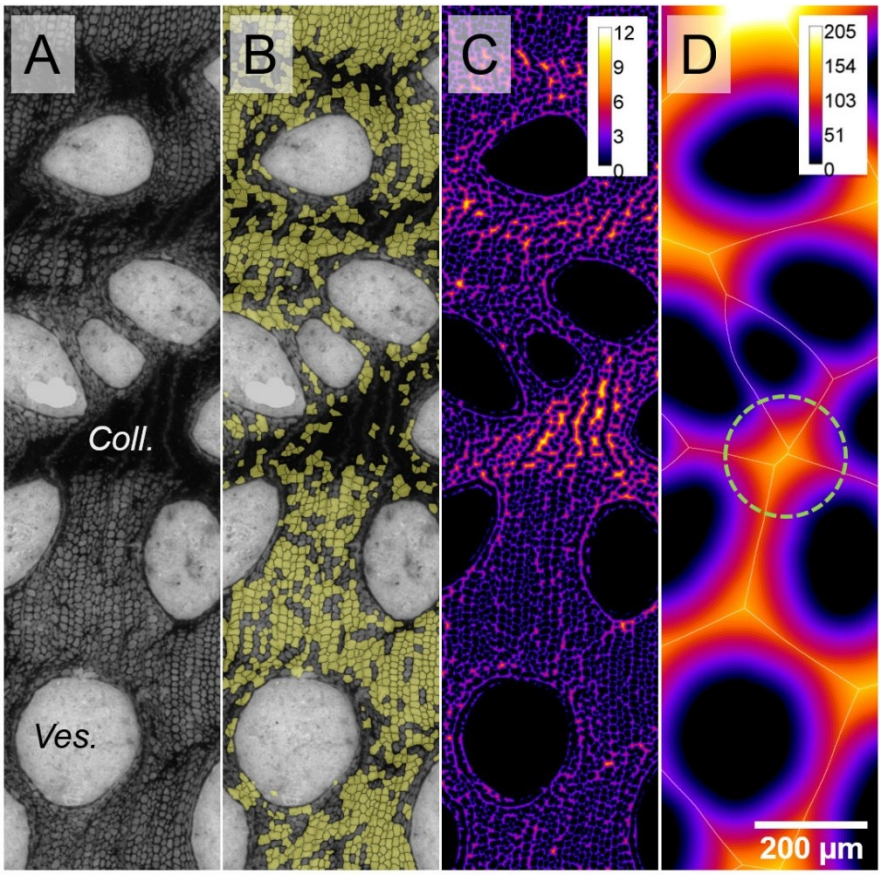

Figure 2. Image analysis of a selected region of an oven-dried sample of *E. nitens*. (A) Greyscale image of cell detail with dark regions of cell collapse (Coll.) and vessels (Ves.). (B) Overlay (yellow) of cells. (C) Map of cell wall thickness (colour scale in µm). (D) Map of distances between vessels (colour scale in µm) with lines in white (farthest positions from vessel lumens) used to determine vessel-free diameters (example in green).

Results

Good image quality was generally achieved but required care being taken during sample preparation. Cell detail and checks were sufficiently preserved for the analysis of wood morphology (Fig 1). Block-face imaging avoided distortion due to sectioning.

Combined maps of vessel distribution, cell lumen deformation, and cell collapse for one selected tree (Fig. 3D-F) show largely undeformed cell lumens in the air-dried sample (green-coloured regions, Fig. 3D) with greater deformation (magenta) mostly associated with higher concentrations of vessels. The kiln-dried sample had increased deformation associated with the vessels (Fig. 3E) and the oven-dried sample showed tangential bands of cell collapse, predominantly on the latewood side of the growth ring (Fig. 3F). In the unprocessed images, the latewood is seen as dark bands due to the increased density (increased wall area, decreased cell perimeter). The maps show that in the oven-dried sample (Fig. 3F) the dark colouration is also due to increased densification resulting from cell collapse. In places, there is a diagonal alignment of regions of cell deformation related to the vessels (Fig. 3H), possibly related to shear stresses generated during timber processing.

Maps also show the oblique alignment of vessels generally expected in *E. nitens* (Dadswell, 1972). In *Eucalyptus*, vessels may be absent in the beginning of the earlywood and tend to be smaller in the latewood (Dadswell, 1972).

There were large differences in the degree of cell collapse due to drying treatment but little significant difference due to position in the growth ring within a drying treatment, although there were indications that collapse was greater between 50-70% across the growth ring for the Air and Kiln drying treatments.

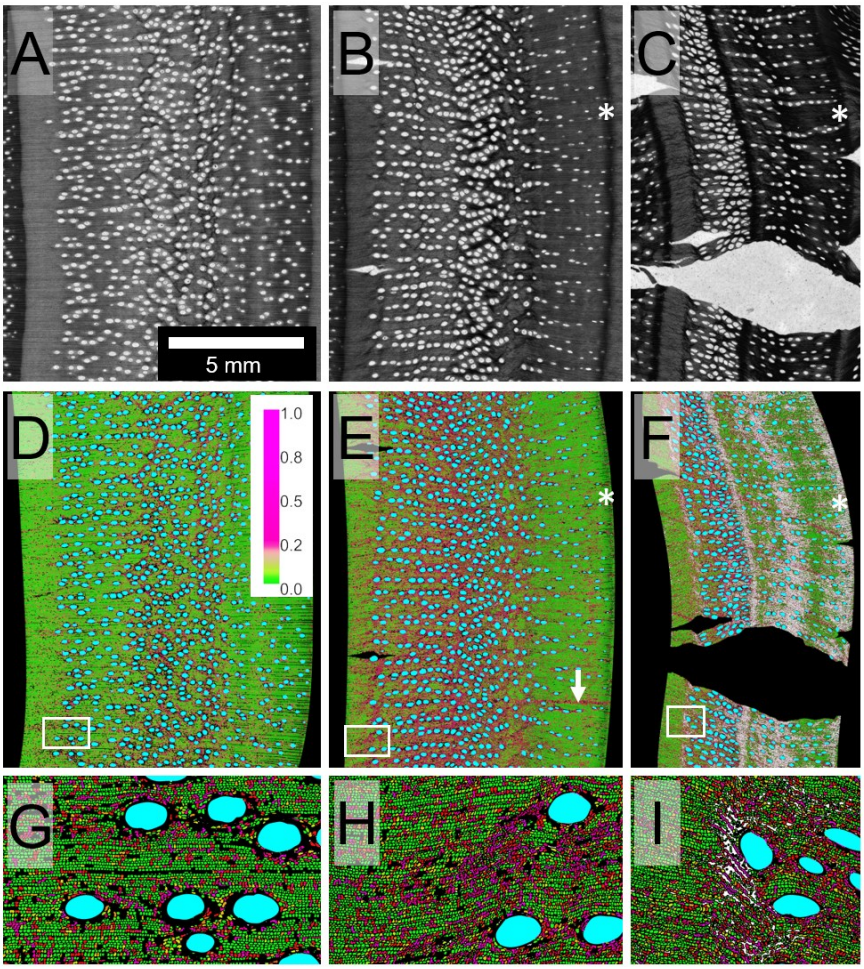

Figure 3. Growth ring images. Earlywood is on the left. Stitched, unprocessed images of (A) Air-dried (B) Kiln-dried (C) Oven-dried. (D) to (I) after image analysis with vessels in cyan. The green-magenta-white colours represent cell lumen deformation with undeformed lumens in green and collapsed cells in white. (G) to (I) are the regions in the white boxes in (D) to (F) respectively. Asterisks (*) show dark bands of latewood in (B) and (C) that show cell collapse in (F) but little deformation or collapse in (E). The arrow in (E) is a stitching artefact.

Discussion

The investigation of wood anatomy and morphology over large regions of investigation better enables the analysis of spatial relationships between them. Some challenges of sectioning large woody specimens can be overcome by sanding and polishing followed by imaging of the exposed block-face (Cerre, 2016; Gärtner, *et al*., 2014; Gärtner & Nievergelt, 2010). The microscopic analysis of drying-induced cell collapse in wood has not been extensively investigated, largely due to difficulties in sample preparation (Yang & Liu, 2018). Analysis that quantifies the position and magnitude of collapse is even rarer.

Often microscopic analysis of drying effects on wood cells is limited to qualitative analysis of selected regions using scanning electron microscopy (Bariska, 1992; Yang & Liu, 2021). Or, where quantification is performed, it is often used to determine the relative effects of moisture on earlywood and latewood (Derome, *et al.*, 2011; Ma & Rudolph, 2006).

There is no strong relationship between cell collapse and position within the growth ring. Where collapse does seem slightly more prevalent, it is in the middle part of the growth ring corresponding to the highest vessel area fraction. This agrees with Chafe (1985) who showed the relationship between cell collapse and high moisture content was greater than it was with low density alone. The presence of water-saturated cells is a requirement for drying-induced cell collapse (Kauman, 1964) and plants invest considerable resources into maintaining the hydraulic integrity of their vascular system (Pfautsch, *et al.*, 2018).

Conclusions

As wood is a composite material, its spatial relationships and complexity need to be taken into account to understand the variability of properties. Mosaic microscopy combined with image analysis at the cellular level and spatial analysis provides the opportunity to characterise a large number of features over large regions. Block-face imaging of polished wood samples using a stereo microscope provided sufficient resolution to measure cell dimensions and drying effects over a wide field of view.

Drying treatment had a significant effect on profiles of cell collapse and vessel shape and size indicating that drying effects vary in relation to position. This kind of detailed spatial analysis enables the investigation of collapse phenomena over size-scales more representative of the scale at which they occur and at the scale at which they cause issues during timber processing.

References

Bariska, M. (1992). Collapse phenomena in eucalypts. *Wood Science and Technology, 26*(3), 165-179. doi:10.1007/BF00224290

Cerre, J. C. (2016). Incident light microphotography at high depth of focus. *IAWA Journal, 37*(3), 506-510. doi:10.1163/22941932-20160149

Chafe, S. C. (1985). The distribution and interrelationship of collapse, volumetric shrinkage, moisture content and density in trees of *Eucalyptus regnans* F. Muell. *Wood Science and Technology, 19*(4), 329-345. doi:10.1007/BF00350810

Dadswell, H. E. (1972). *The anatomy of Eucalypt woods*.

Dawson, B., Pearson, H., Kimberley, M. O., Davy, B., & Dickson, A. R. (2020). Effect of supercritical CO_2 treatment and kiln drying on collapse and internal checking in *Pinus radiata* and *Eucalyptus nitens* wood. *European Journal of Wood and Wood Products, 78*(2), 209-217. doi:https://doi.org/10.1007/s00107-020-01500-5

Derome, D., Griffa, M., Koebel, M., & Carmeliet, J. (2011). Hysteretic swelling of wood at cellular scale probed by phase-contrast X-ray tomography. *Journal of Structural Biology, 173*(1), 180-190. doi:10.1016/j.jsb.2010.08.011

Dickson, A., & Dawson, B. (2020). Using cell cross-section dimensions and digital image correlation to evaluate drying shrinkage and collapse in *Eucalyptus nitens* wood. *BioResources, 15*(3), 6149-6164. doi:10.15376/biores.8.3.6149-6164

Dickson, A., Nanayakkara, B., Sellier, D., Meason, D., Donaldson, L., & Brownlie, R. (2017). Fluorescence imaging of cambial zones to study wood formation in *Pinus radiata* D. Don. *Trees, 31*(2), 479-490. doi:10.1007/s00468-016-1469-3

Gärtner, H., Lucchinetti, S., & Schweingruber, F. H. (2014). New perspectives for wood anatomical analysis in dendrosciences: The GSL1-microtome. *Dendrochronologia, 32*(1), 47-51. doi:10.1016/j.dendro.2013.07.002

Gärtner, H., & Nievergelt, D. (2010). The core-microtome: A new tool for surface preparation on cores and time series analysis of varying cell parameters. *Dendrochronologia, 28*(2), 85-92. doi:10.1016/j.dendro.2009.09.002

Kauman, W. (1964). *Cell collapse in wood.* CSIRO Division of Forest Products.

Kauman, W. G. (1960). Contribution to the theory of cell collapse in wood: Investigations with Eucalyptus regnans. *Australian Journal of Applied Science, 11*(1), 122-145. doi:http://dx.doi.org/10.4067/S0718-221X2002000100007

Ma, Q., & Rudolph, V. (2006). Dimensional Change Behavior of Caribbean Pine Using an Environmental Scanning Electron Microscope. *Drying Technology, 24*(11), 1397-1403. doi:10.1080/07373930600952743

Nanayakkara, B., Dickson, A. R., & Meason, D. F. (2019). Xylogenesis of *Pinus radiata* D. Don growing in New Zealand. *Annals of Forest Science, 76*(3). doi:10.1007/s13595-019-0859-2

Pfautsch, S., Aspinwall, M. J., Drake, J. E., Chacon-Doria, L., Langelaan, R. J. A., Tissue, D. T., Tjoelker, M. G., & Lens, F. (2018). Traits and trade-offs in whole-tree hydraulic architecture along the vertical axis of *Eucalyptus grandis*. *Annals of Botany, 121*(1), 129-141. doi:10.1093/aob/mcx137

Preibisch, S., Saalfeld, S., & Tomancak, P. (2009). Globally optimal stitching of tiled 3D microscopic image acquisitions. *Bioinformatics, 25*(11), 1463-1465. doi:10.1093/bioinformatics/btp184

Satchell, D. (2016). *Eucalyptus nitens* for solid timber – silk purse or sow's ear? *NZ Journal of Forestry, 60*(4), 33-36.

Wickham, H. *ggplot2: Elegant graphics for data analysis*. Retrieved from https://github.com/hadley/ggplot2-book

Wickham, H., François, R., Henry, L., & Müller, K. *dplyr: A grammar of data manipulation. R package version 0.8.3*. Retrieved from https://CRAN.R-project.org/package=dplyr

Yang, L., & Liu, H. (2018). A review of eucalyptus wood collapse and its control during drying. *BioResources, 13*(1), 2171-2181. doi:10.15376/biores.13.1.Yang

Yang, L., & Liu, H. (2021). Study of the collapse and recovery of *Eucalyptus urophydis* during conventional kiln drying. *European Journal of Wood and Wood Products, 79*(1), 129-137. doi:10.1007/s00107-020-01614-w